Biochimica et Biophysica Acta 1840 (2014) 476–484

Contents lists available at ScienceDirect

Biochimica et Biophysica Acta

journal homepage: www.elsevier.com/locate/bbagen

Evaluation of chitosan nanoformulations as potent anti-HIV therapeutic systems

Lakshmi Narashimhan Ramana [a], Shilpee Sharma [b], Swaminathan Sethuraman [a], Udaykumar Ranga [b], Uma Maheswari Krishnan [a,*]

[a] Centre for Nanotechnology & Advanced Biomaterials (CeNTAB), SASTRA University, Thanjavur, India
[b] HIV-AIDS Laboratory, Molecular Biology and Genetics Unit, Jawaharlal Nehru Centre for Advanced Scientific Research (JNCASR), Bangalore, India

ARTICLE INFO

Article history:
Received 16 April 2013
Received in revised form 30 September 2013
Accepted 2 October 2013
Available online 9 October 2013

Keywords:
Nanocarrier
Chitosan
Saquinavir
Antiretroviral

ABSTRACT

Background: Antiretroviral Therapy (ART) is currently the major therapeutic intervention in the treatment of AIDS. ART, however, is severely limited due to poor availability, high cytotoxicity, and enhanced metabolism and clearance of the drug molecules by the renal system. The use of nanocarriers encapsulating the antiretroviral drugs may provide a solution to the aforementioned problems. Importantly, the application of mildly immunogenic polymeric carrier confers the advantage of making the nanoparticles more visible to the immune system leading to their efficient uptake by the phagocytes.
Methods: The saquinavir-loaded chitosan nanoparticles were characterized by transmission electron microscopy and differential scanning calorimetry and analyzed for the encapsulation efficiency, swelling characteristics, particle size properties, and the zeta potential. Furthermore, cellular uptake of the chitosan nanocarriers was evaluated using confocal microscopy and Flow cytometry. The antiviral efficacy was quantified using viral infection of the target cells.
Results: Using novel chitosan carriers loaded with saquinavir, a protease inhibitor, we demonstrate a drug encapsulation efficiency of 75% and cell targeting efficiency greater than 92%. As compared to the soluble drug control, the saquinavir-loaded chitosan carriers caused superior control of the viral proliferation as measured by using two different viral strains, NL4-3 and Indie-C1, and two different target T-cells, Jurkat and CEM-CCR5.
Conclusion: Chitosan nanoparticles loaded with saquinavir were characterized and they demonstrated superior drug loading potential with greater cell targeting efficiency leading to efficient control of the viral proliferation in target T-cells.
General significance: Our data ascertain the potential of chitosan nanocarriers as novel vehicles for HIV-1 therapeutics.

© 2013 Elsevier B.V. All rights reserved.

1. Introduction

Acquired Immune Deficiency Syndrome (AIDS) is a dreadful immune disorder caused by the human immunodeficiency virus (HIV) that has resulted in the death of millions across the globe. Currently, more than 36 million people are infected with HIV globally, with a large percentage living in the developing countries [1]. The current treatment employs a combination regimen known as Highly Active Anti-Retroviral Therapy (HAART) [2]. There are five major classes of anti-retroviral drugs currently approved for treatment of AIDS. These are reverse transcriptase inhibitors that include the nucleoside reverse transcriptase inhibitors (NRTIs), nucleotide reverse transcriptase inhibitors (NtRTIs) and non-nucleotide reverse transcriptase inhibitors (NNRTIs), protease inhibitors (PIs), fusion inhibitors and integrase inhibitors [3]. These drugs act at different phases of the viral life cycle [4]. Protease inhibitors target the viral protease that is involved in the cleavage of the GAG-POL precursor responsible for the production of viral enzymes necessary for the viral proliferation [5]. Inhibition of the viral proliferation at the later stages is critical to prevent viral maturation resulting in the formation of the immature and non-infectious virions [6]. Currently, there are eight protease inhibitors approved by the FDA among which saquinavir is the most potent.

Conventional saquinavir therapy is not quite effective due to its poor bioavailability [7]. The poor bioavailability of saquinavir is mainly attributed to a group of MDR1 (multi-drug resistant 1) proteins, the P-gp mediated efflux system, which causes the elimination of the drug due to its resemblance with the substrate analog of the P-gp mediated system [8,9]. The accelerated drug efflux results in the low intracellular concentration of the drug in the target cells. Yet another mechanism proposed for the low bioavailability of saquinavir is its metabolism by the hepatic system and small intestine leading to the rapid clearance of the drug

* Corresponding author at: Departments of Chemistry, Bioengineering & Pharmacy, Centre for Nanotechnology & Advanced Biomaterials (CeNTAB), School of Chemical & Biotechnology, SASTRA University, Thanjavur 613 401, Tamil Nadu, India. Tel.: +91 4362 264101x3677; fax: +91 4362 264120.
E-mail address: umakrishnan@sastra.edu (U.M. Krishnan).

0304-4165/$ – see front matter © 2013 Elsevier B.V. All rights reserved.
http://dx.doi.org/10.1016/j.bbagen.2013.10.002

[10]. It is reported that the cytochrome P450 isoenzymes, especially the CYP3A4, are involved in the biotransformation of the drug leading to its rapid clearance and low availability thus affecting its efficacy. The poor bioavailability of saquinavir requires an increase in the dosage, and in the absence of which rapid emergence of drug resistance is a possible outcome [11]. Apart from the bioavailability issues, the use of saquinavir is also accompanied by several adverse effects including dizziness, nausea, arrhythmia, etc. The nanotechnology enabled platforms such as dendrimers [12], liposomes [13], polymeric nanoparticles [14], etc., could alleviate the limitations of the use of saquinavir, thereby enhancing the therapeutic potential of saquinavir.

Only a few studies attempted to enhance the bioavailability of saquinavir using the nanocarrier-mediated delivery strategies. A solid lipid nanoparticle was used to improve the bioavailability of saquinavir although its efficacy on reducing the viral load was not investigated [15]. A poly(ethylene glycol) modified poly(caprolactone) (PEO-PCL) nanoparticle system prepared using the solvent displacement method was found to enhance the intracellular concentrations of saquinavir suggesting improved cell uptake of the drug [16]. Using an in vitro cell model for the blood–brain barrier and HIV-1 infection, the saquinavir-loaded and transferrin-conjugated quantum rods were shown to cross the barrier alluding to improved efficacy of the drug [17]. Oil in water emulsions of saquinavir were found to exhibit superior oral bioavailability [18]. Similarly, hydroxylpropyl-β-cyclodextrin and poly(alkyl cyanoacrylate) nanoparticles have also shown improvement in the bioavailability of saquinavir [19]. Cationic submicron emulsions of saquinavir were shown to improve the oral absorption of saquinavir although its effect on the viral proliferation was not studied [20]. We previously developed a liposomal delivery system for saquinavir that exhibited excellent cell uptake properties [21].

In the present work, we report a chitosan-based nanodelivery strategy for saquinavir. The choice of chitosan, a natural polymer, is due to its immunogenicity and its anti-microbial properties [22]. The cationic surface of chitosan is expected to contribute to its superior targeting efficacy to negatively charged cells. Furthermore, the polycationic nature of chitosan is expected to favor the deposition of the complement proteins on the nanoparticles resulting in their uptake by the macrophages through complement receptors [23]. The macrophages serve as HIV-1 reservoirs thus efficient drug delivery to these cells via chitosan could be an added advantage. The drug release from the chitosan carriers could be accentuated in the acidic endosome due to extensive protonation and destabilization of the polymer matrix [24].

2. Materials & methods

2.1. Materials

Sodium dihydrogen phosphate and disodium hydrogen phosphate were purchased from Merck Chemicals, India. Chitosan (M.W. = 140 kDa, 85% deacetylated) was a kind gift from India Sea Foods, Kochi, India. Saquinavir was a kind gift from M/s Hetero drugs, India. Sodium tripolyphosphate (TPP) was purchased from Lobachemie, India. RPMI 1640media and fetal bovine serum were procured from Sigma-Aldrich, USA.

2.2. Preparation of blank and saquinavir loaded nanoparticles

Chitosan nanoparticles were prepared by the ionic gelation technique. A 1000 μg (w/v) solution of chitosan dissolved in 1% acetic acid was stirred with 0.1% (w/v) TPP. The appearance of the turbidity was taken as an indicator of the formation of the chitosan nanoparticles [25]. For the preparation of saquinavir loaded chitosan, 1 mg/ml of the chitosan solution and 1 mg/ml of the drug were dissolved in the phosphate buffered saline (PBS) (1:1 chitosan:saquinavir) followed by the addition of the TPP until the appearance of a turbid solution with constant stirring. The samples were centrifuged at 18,000 rpm and washed thrice to remove the unencapsulated saquinavir. The samples were lyophilized and stored in a cool dry place before use. 1% w/v sucrose was used as the cryoprotectant during lyophilization. The Alexa Fluor 647 loaded chitosan nanoparticles were prepared following the same protocol employed for preparation of saquinavir-loaded nanoparticles.

2.3. Morphology of chitosan

The ultra fine structure of the blank chitosan and saquinavir loaded chitosan was observed using field emission transmission electron microscopy (JEM2100 F, JEOL, Japan). 500 μg of the lyophilized drug-loaded and blank chitosan nanoparticles was taken and dispersed in 500 μl of PBS and placed on a copper grid coated with carbon. The sample was left overnight for drying and then imaged.

2.4. Physico-chemical characterization

The saquinavir loaded chitosan solution was centrifuged at 20,000 rpm for 20 min to separate the drug loaded with chitosan as pellet and the supernatant containing the unencapsulated saquinavir. The blank corrections were carried out using TPP and the absorbance of the unencapsulated drug was measured using the UV–vis spectrophotometer (Lambda 25, Perkin Elmer, USA) at 239 nm [26]. The absorbance was converted to concentration using a standard curve.

The encapsulation efficiency was calculated as:

$$\text{Encapsulation Efficiency} = \frac{\textit{Total Drug} - \textit{Unencapsulated Drug}}{\textit{Total Drug}} * 100.$$

1000 μg of blank and drug loaded chitosan nanoparticles dispersed in 1000 μl PBS was used for the particle size and zeta potential measurements. The particle size and zeta potential of the samples were measured using the Zeta sizer (Nano-ZS, Malvern, UK). The blank chitosan and drug loaded chitosan were dispersed in 1 ml PBS and the mean particle size and zeta potential were measured.

The glass transition temperature of the blank chitosan and drug loaded samples was measured using a differential scanning calorimeter (DSC, Q20, TA Instruments, USA). Six milligrams of the sample was kept in an aluminum pan along with the standard reference aluminum and the glass transition temperature was measured between the range of 10 °C and 180 °C at a scan rate of 10 °C/min under nitrogen atmosphere.

100 mg of placebo chitosan was placed in a dialysis bag and the dialysis bag was immersed in the 200 ml of buffer solution that was maintained at 37 °C. The swelling studies were carried out at different pH values (5.5, 7.4 and 9.0). After 1 h of incubation, sample was removed from the buffer medium and the excess moisture was removed gently using tissue paper followed by weighing. The swelling ratio was calculated using the following formula:

$$SW = \frac{WT - WO}{WO} * 100$$

where SW represents the swelling ratio, WO represents the original dry weight of the blank chitosan and WT represents the weight of the sample at time t.

2.5. Release kinetics

1000 μg of the drug-loaded chitosan was taken and dispersed in 4 ml of PBS and then the entire sample was placed in a dialysis bag, which was then sealed at both the ends and immersed in 4 ml of PBS buffer solution. Each experiment was carried out in triplicate. The PBS was removed at a predetermined interval of time and replaced with the fresh media of the same volume. The procedure was repeated for different pH values (5.5, 7.4 and 9.0) and the absorbance of the collected PBS was measured at 239 nm using a UV–visible spectrophotometer

(Lambda 25, Perkin Elmer, USA). The absorbance was converted to concentration using a standard curve.

2.6. In vitro protein adsorption

1000 μg of the chitosan nanoparticles (blank or drug-loaded) was dispersed in PBS and incubated with 1000 μg of FBS protein at 37 °C for 12 h. The sample was then centrifuged at 18,000 rpm to sediment the chitosan nanoparticles with the adsorbed layer of proteins. The supernatant was used for estimating the unadsorbed protein using Lowry's method. The intensity of the colored product obtained after treating the samples with Lowry's reagent was quantified at 660 nm using a UV–visible spectrophotometer (Lambda 25, Perkin Elmer, USA).

2.7. Evaluation of the cellular uptake

2.7.1. Evaluation of chitosan delivery using flow cytometry and confocal microscopy

Jurkat T-cells, 0.5×10^5 cells per assay, were incubated in 200 μl of plain RPMI containing plain chitosan (PC) or Alexa Fluor 647 (AFL) loaded chitosan nanoparticles, normalized for 300 or 600 μg of total chitosan nanoparticles. The cells were incubated at 37 °C in a 5% CO_2 incubator for 30 min and washed twice in 1X PBS. Cells were stained using the Live/Dead Fixable Green Stain Kit (Cat. No: L-23101, Molecular Probes, Invitrogen Detection Technologies, Carlsbad, CA, USA) for 30 min in the dark as per the manufacturer's instructions. Cells were washed twice in 1X PBS and fixed in 400 μl of 1% paraformaldehyde before the acquisition using a FACS Calibur flow cytometer. Data were analyzed using the BD CellQuest Pro software.

2.7.2. The confocal analysis

Jurkat T-cells, 50,000 cells suspended in 200 μl of RPMI medium, were incubated in the presence of 300 μg of Alexa Fluor 647 loaded chitosan nanoparticles. The cells were incubated at 37 °C in a 5% CO_2 incubator for 30 min, centrifuged at 2000 rpm and the pellet was washed with 400 μl of PBS. The cells were stained with the Hoechst 33258 dye (5 μg/ml) for 30 min at room temperature. Cells were washed with PBS and then mounted in 70% glycerol for imaging using the laser scanning confocal microscope (FV1000, Olympus, Japan).

2.7.3. Cellular uptake of the plain saquinavir and saquinavir loaded chitosan

Jurkat T-cells, 50,000 cells were suspended in 200 μl of RPMI medium and incubated with 100 μg, 300 μg and 600 μg of saquinavir-loaded chitosan nanoparticles containing 72 μg, 216 μg and 432 μg saquinavir respectively. The results were compared with those for cells incubated with the same quantity of free saquinavir for comparison. The cells were incubated at 37 °C in a 5% CO_2 incubator for 30 min and centrifuged at 2000 rpm. The resultant pellet was treated with cell lysis buffer and then incubated for 30 min. The absorbance of the samples was measured at 239 nm using a UV–vis spectrophotometer (Lambda 25, Perkin Elmer, USA). The absorbance was converted to concentration using the standard curve.

2.8. In vitro antiviral efficacy

2.8.1. Cell culture

The human embryonic kidney HEK293T cells were grown in Dulbecco's modified Eagle's medium (Sigma-Aldrich, St. Louis, USA) supplemented with 10% heat inactivated fetal bovine serum (Biological Industries, Israel), 2 mM glutamine, 100 U/ml penicillin G, and 100 g/ml streptomycin. The Jurkat and CEM-CCR5 cells were cultured in RPMI 1640 medium (Sigma, St. Louis, Missouri, USA) supplemented with 10% fetal bovine serum. All the cells were maintained at 37 °C in an incubator in the presence of 5% CO_2.

2.8.2. Production of the viral stocks

The viral stocks were prepared using HEK293T cells by transiently transfecting the cells with plasmid DNA containing the HIV-1 molecular clones NL4-3 (subtype B) or Indie-C1 (subtype C). Cells seeded in 100 mm dishes at a low confluency were transfected 24 h later with 10 μg of the viral plasmid DNA. The culture medium was changed after 6 h of incubation. The culture supernatant, containing the virus was harvested at 60 h, passed through a 0.45 μm filter and stored in multiple aliquots at −80 °C until use. The concentration of the viral core protein p24 in the viral stocks was measured using a commercial ELISA kit (Cat. No: 5421, Advanced BioScience Laboratories, Kensington, MD, USA) following the manufacturer's instructions. Viral stock of 5 ng p24 equivalent was used for the infection of CEM-CCR5 or Jurkat-T cell lines.

2.8.3. Viral inhibition assay

The in vitro viral inhibition was evaluated in CEM-CCR5 or Jurkat T-cell lines. The cells suspended in plain RPMI medium and seeded in 24-well culture plates, 0.5×10^6 per well, were exposed to six different concentrations (0, 4, 16, 64, 256 and 1024 ng/500 μl) of saquinavir (SQV) in the soluble form or as drug loaded in chitosan nanoparticles (SQV_{NP}). The total amount of chitosan used in the experiment was normalized to 1400 ng using blank chitosan nanoparticles. Cells in 400 μl of plain medium were incubated for 30 min at 37 °C and in the presence of 5% CO_2. Following the incubation, CEM-CCR5 and Jurkat-T cells were infected with Indie-C1 or NL4-3 viruses, respectively, by adding 5 ng of the p24 equivalent of the virus to appropriate wells. The final volume in each well was made up to 500 μl by adding a complete medium supplemented with fetal bovine serum and DEAE dextran, and the latter was used at a final concentration of 8 μg/ml. Cells were incubated for 6 h, at 37 °C and in the presence of 5% CO_2. The cells were centrifuged at 2000 rpm and the cell pellet was washed three times with 500 μl of 1X PBS (pH 7.2). The cells resuspended in 1 ml of complete medium were incubated for 3 days at 37 °C in the presence of 5% CO_2. All the assays were performed in duplicate wells and repeated two times. The amount of viral antigen p24 secreted into the medium was monitored using a commercial kit (Cat. No: 5421, Advanced BioScience Laboratories, Kensington, MD, USA). One hundred microliters of cell-free supernatants of the infected cultures were harvested at three different time points (24, 48 and 72 h) and stored frozen in aliquots in a deep freezer until the analysis. An unpaired two-tailed *t*-test was performed using the Graphpad Prism 5 software to determine the significance of differences in the magnitude of viral inhibition between the groups.

2.9. Statistical analysis

The data are represented as mean ± standard deviation ($n = 3$). The analysis of variances was calculated using two-way ANOVA and the Tukey test was performed to test the level of significance for cell culture assay. A two-way ANOVA test was performed using the Graphpad Prism 5 software to determine the significance of differences in the magnitude of viral inhibition between the groups.

3. Results and discussion

3.1. Encapsulation efficiency

The encapsulation of saquinavir into chitosan was achieved through passive loading and Table 1 shows the encapsulation efficiency of the drug at various chitosan to drug ratios. Chitosan presents a hydrophilic matrix that can load hydrophilic drugs more effectively. Saquinavir is a derivative of the amino acid asparagine and retains some hydrophilic character in spite of the aromatic modifications. Its aqueous solubility increases in acidic pH and as the encapsulation is carried out at pH 5.5, about 75% of saquinavir encapsulation is achieved in chitosan. As the ratio of chitosan to drug is increased from 1:1 to 2:1, a marginal increase in the encapsulation efficiency is observed beyond which no

Table 1
Encapsulation efficiency of saquinavir at different chitosan:drug ratios.

Chitosan:Saquinavir	Encapsulation efficiency (%)
1:1	72.24 ± 0.69
1:2	74.34 ± 1.47
1:3	76.99 ± 2.02[a*]
2:1	75.82 ± 1.74[a*]
3:1	77.73 ± 4.33[a*]
4:1	78.70 ± 2.23[a*]

[a] The data is compared with the 1:1 ratio of drug:chitosan.
* $p < 0.05$.

Table 2
Zeta potential and particle size of blank chitosan and saquinavir loaded chitosan.

Nanoparticle	Size (nm)	Zeta potential (mV)
Blank chitosan	132 ± 2.91	30.6 ± 1.42
Saquinavir loaded chitosan	211 ± 11.50*	24.4 ± 1.02

* $p < 0.05$.

further enhancement is obtained. The increase in the drug to chitosan ratio also results in a very small increase in the encapsulation efficiency. However, the lack of substantial increase in the encapsulation efficiency from the values obtained in the 1:1 chitosan to drug ratio suggests that the chitosan matrix has been saturated with the drug. Hence this ratio was used for further experiments.

3.2. Characterization of the plain and saquinavir-loaded chitosan nanoparticles

The shape of the blank and saquinavir-loaded chitosan nanoparticles was investigated using high-resolution transmission electron microscopy (HR-TEM) (Fig. 1). Both the blank as well as drug-loaded chitosan systems exhibited a smooth spherical morphology. However, the size of the drug-loaded system was found to be nearly twice than that of the blank chitosan system.

Table 2 shows the particle size and the zeta potential of the blank and drug loaded chitosan nanoparticles. The size of the saquinavir loaded chitosan nanoparticles exhibited a significant increase indicating the incorporation of the drug. The increase in size may be attributed to the localization of the drug in the interior of the matrices of chitosan [27]. No significant changes were observed in the particle sizes of the blank chitosan after lyophilization. The polydispersity index of the chitosan nanoparticles was around 0.166–0.199. The zeta potential of chitosan exhibited a positive value owing to the amino groups present in chitosan. The positive zeta potential prevents the aggregation of chitosan nanoparticles as is evident from the transmission electron micrographs (Fig. 1). The zeta potential of chitosan reduces on encapsulation of saquinavir and the reduction in the zeta potential indicates the presence of some drug molecules on the surface of chitosan, which masks the surface charges thereby lowering the zeta potential [28]. The positive zeta potential of the drug-loaded chitosan nanoparticles may prove to be beneficial in vivo since saquinavir loaded in cationic microspheres exhibits superior absorption of the drug by the intestine [29].

3.3. Thermal analysis

The drug–matrix interactions were investigated by determining the phase transition temperature of the chitosan carrier in the absence and presence of saquinavir. Fig. 2 shows the melting point curves of the blank chitosan and saquinavir-loaded chitosan. The melting point curves of the blank chitosan and the saquinavir loaded chitosan show endothermic peaks at 75 °C and 95 °C respectively. The positive shift in the transition temperature in the drug loaded system suggests extensive interactions between saquinavir and chitosan, possibly through hydrogen bonds which decrease the flexible segmental motion of the chains [30]. The appearance of a broad peak for the blank chitosan may be ascribed to moisture throughout the matrix [31]. Interestingly, the width of this peak decreases in the presence of saquinavir suggesting that the localization of the drug in the interior of the chitosan reduces the water content through displacement [32].

3.4. Swelling ratio

The swelling profiles at different pH values for chitosan nanoparticles are presented in Fig. 3A. The extent of swelling of the chitosan nanoparticles is expected to strongly influence the rate of drug release. The percentage of swelling after 1 h in pH 5.5, 7.4 and 9.0 for chitosan nanoparticles was found to be 168%, 42% and 25% respectively. The amino groups in chitosan get protonated at acidic pH resulting in repulsive forces between the chains. This leads to influx of solvated counter ions from the medium causing the swelling. The intrusion of water molecules and the subsequent swelling disrupts few hydrogen bonds leading to extension of the chains and higher hydrodynamic volumes [33]. Beyond pH 7.0, the $-NH_3^+$ groups get deprotonated to form the basic $-NH_2$ form reducing the influx of charged solvated species into the chitosan matrix. Also, the amino groups are involved in extensive intermolecular hydrogen bonding with the polymeric chains causing them to

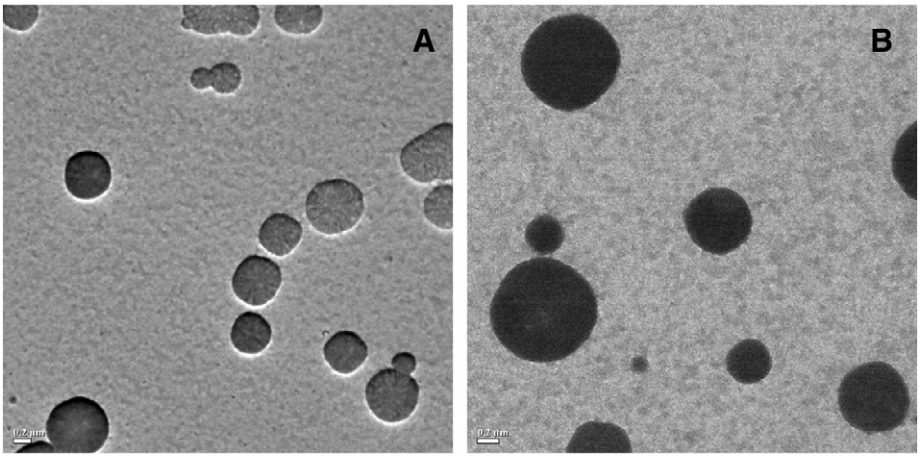

Fig. 1. Transmission electron micrographs of [A] blank chitosan and [B] saquinavir-loaded chitosan.

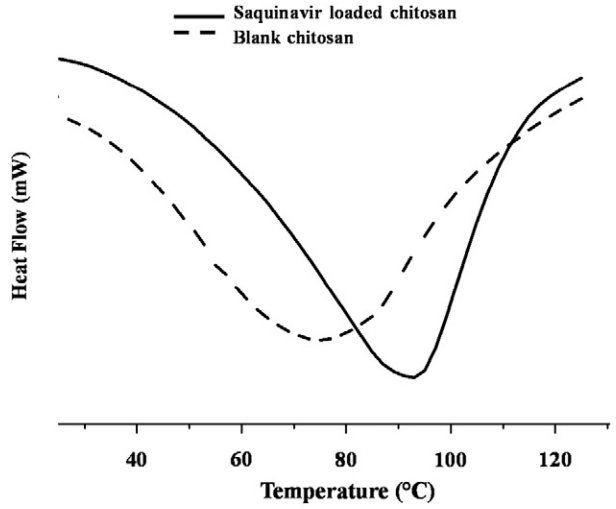

Fig. 2. Phase transition of blank chitosan and saquinavir loaded chitosan.

associate more closely. Consequently, the water permeation is retarded and hence the swelling ratio decreases progressively with the increase in pH. The magnitude of swelling does not increase beyond 1 h indicating the onset of equilibrium in the system.

3.5. In vitro release profiles of saquinavir

Fig. 3B depicts the release profiles of saquinavir from chitosan at different pH values. It is observed that the release profiles match the trend followed during swelling of chitosan at different pH values. The release of the drug was found to be fastest in acidic pH where the swelling was also found to be the highest. The slowest release profile was observed at pH 9.0 while the release at pH 7.4 was intermediate between the two. The initial burst release was prominent in the acidic pH. About 62% of the drug was released within 2 h in pH 5.5 compared to 12% and 7% at pH 7.4 and 9.0 respectively for the same duration. The complete drug release in acidic medium occurred in 12 h when compared to 48 and 36 h for the total release of saquinavir from chitosan in pH 7.4 and 9.0 respectively. Faster drug release in the acidic pH can be directly correlated with the enhanced swelling of chitosan caused by its polycationic nature resulting in the expulsion of the drug from the matrix. Further, the enhanced drug release from the chitosan matrix in acidic pH may also be due to the increase in solubility of chitosan in acidic pH [34]. The drug release is retarded in neutral and alkaline pH conditions due to the limited solubility of the chitosan at pH 7.4 and 9.0 [35]. Also the deprotonation of the amino groups in chitosan favors the formation of hydrogen bonds, both interchain and intrachain, thereby lowering its swelling capacity and leading to minimal drug release.

In order to understand the possible mechanism of release of saquinavir from the chitosan matrix, the release data at various pH values was

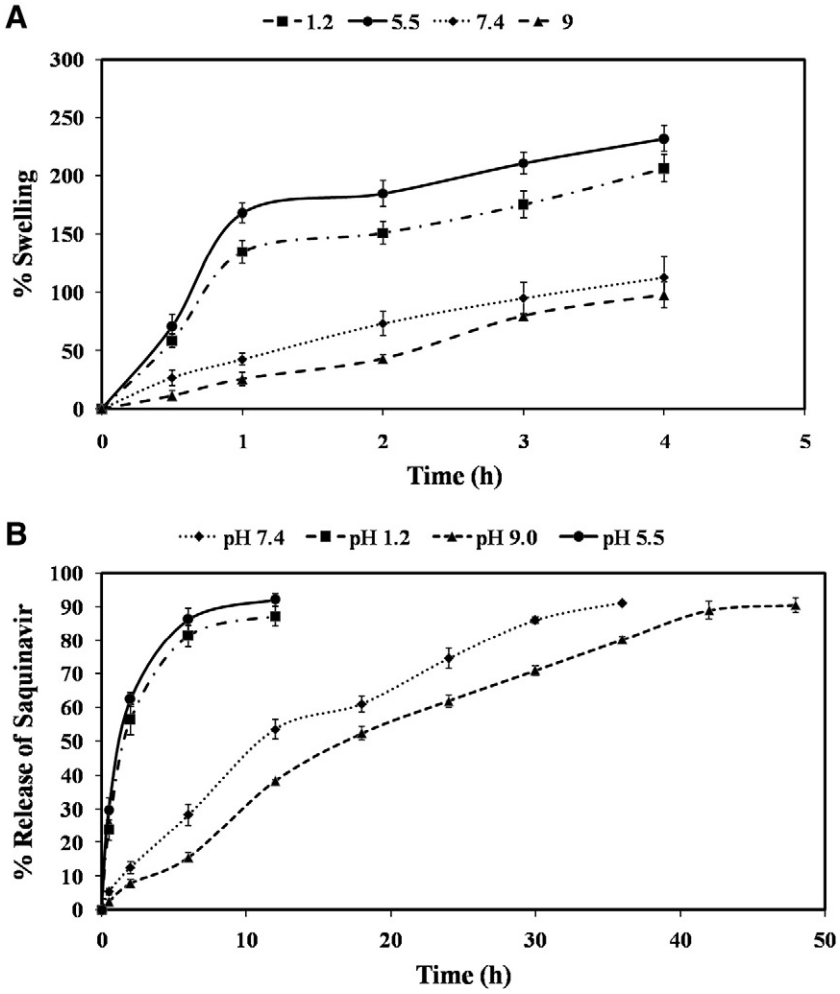

Fig. 3. [A] Percentage swelling of chitosan at different pH values i.e. 1.2, 5.5, 7.4 and 9.0 and [B] in vitro release kinetics of saquinavir at different pH values i.e. 5.5, 7.4 and 9.0.

analyzed using different kinetic models. The kinetic equations used are as follows.

Zero order equation

$f = k_0 \times t$

k_0 = Reaction rate coefficient
t = time

First order equation

$f = 100 \times [1 - e^{-k_1 t}]$

k_1 = Rate constant
t = time

Higuchi model and Weibull model

$f = k_H \sqrt{t}$

k_H = Higuchi dissolution constant
f = Amount of the drug release
t = time
α = Scale parameter describes the time dependence

Korsmeyer–Peppas model

$f = k_{KP} t^n$

k_{KP} = Constant depicting the experimental parameters based on geometry and dosage forms
n = release exponent
f = Amount of the drug release
t = time

Hixson–Crowell model

$f = 100[1 - (1 - k_{HC} t)^3]$

k_{HC} = Constant depicting surface volume relation
f = Amount of the drug release
t = time

Gompertz model

$f = 100 \times e^{\left\{-\alpha e^{[-\beta \times \log(t)]}\right\}}$

t = time
f = Amount of the drug release
β = Shape of the dissolution curve
α = Scale parameter describes the time dependence

Baker–Lonsdale model

$k_{BL} t = {}^3/_2 \left[1 - \left(1 - {}^f/_{100}\right)^{2/3}\right] - {}^f/_{100}$

f = Amount of the drug release
k_{BL} = Release constant
t = time

$f = 100 \times \left\{1 - e^{\left[-\frac{((t-T_l)\beta)}{\alpha}\right]}\right\}$

t = time
f = Amount of the drug release
β = Shape of the dissolution curve

Hopfenberg model

$f = 100 \times e[1 - (1 - k_{HB} \times t)^n]$

k_{HB} = Erosion rate constant
f = Amount of the drug release

t = time

The regression coefficient values obtained for the various kinetic models are listed in Table 3. It is evident that the release profiles for saquinavir from chitosan exhibit good agreement with the Weibull model at all pH conditions suggesting that chitosan presents a matrix-type of drug loading. The zero order kinetics is not obeyed at any pH and the kinetic data fits better for the Korsmeyer–Peppas model than the Higuchi model at all pH conditions, especially at pH > 7. This implies that saquinavir release from the chitosan matrix is a combination of both diffusion as well as erosion. The diffusional exponent values determined from the Korsmeyer–Peppas equation for the saquinavir release from chitosan indicate that at acidic pH, a quasi-Fickian diffusion occurs in the system while at alkaline pH, the diffusion becomes non-Fickian. The anomalous behavior is expected as chitosan also undergoes swelling.

First order release kinetics is obeyed at alkaline pH indicating that the rate of drug release is proportional to the amount of drug present in the matrix. The regression coefficient values for the first order kinetics at acidic pH are below 0.97 indicating that there are other factors that influence the drug release at acidic pH. The release profiles of saquinavir from chitosan at alkaline pH also show agreement with the Hixson–Crowell and Hopfenberg models. This indicates that the erosion processes are more dominant at alkaline pH resulting in a progressive change in the surface area. The agreement with the Hopfenberg model indicates a surface erosion regime operating at the alkaline pH. The release kinetics at all pH conditions agrees well with the Gompertz model suggesting the release of a water-soluble drug from the matrix. Interestingly, the release data at the acidic pH agrees better with the Gompertz model and this may be attributed to the enhanced solubility of saquinavir in acidic pH [36]. The Baker–Lonsdale model that is associated with the release of a drug from a spherical matrix, is found to be followed at pH 5.5 at which the chitosan exhibits maximum swelling.

3.6. In vitro protein adsorption

One of the challenges for a nanoparticle in in vivo conditions is immune recognition, which is triggered through a process of blood protein adsorption on the surface of the nanoparticle known as 'opsonization'. The influence of saquinavir loading on the protein adsorption properties of chitosan nanoparticles was determined and the results are shown in Fig. 4. When the chitosan nanoparticles were incubated in fetal bovine serum for 12 h, the amount of protein adsorbed on the blank chitosan and the saquinavir loaded chitosan nanoparticles was 84% and 67% respectively. Higher values of protein adsorption for blank chitosan arise mainly due to its cationic charge that easily interacts with the negatively charged proteins in the serum, especially albumin [37]. Thus it is evident that chitosan will be easily recognized by the immune system in vivo, which is in agreement with earlier reports [38]. The magnitude of protein adsorption on the chitosan surface has a close correlation with its zeta potential [39]. Higher zeta potential favors greater protein adsorption as in the case of the blank chitosan. The drug loaded chitosan has lower zeta potential, which in turn leads to reduced protein adsorption because of lesser surface charges. As the magnitude of surface charges are bound to change with pH, it is likely that chitosan nanoparticles will attract more proteins in acidic pH when compared with alkaline pH.

3.7. Cellular uptake using confocal microscopy and flow cytometry

The cellular uptake of chitosan nanoparticles loaded with the fluorescent dye Alexa Fluor 647 was qualitatively assessed using laser scanning confocal microscopy and quantitatively assessed using flow cytometry (Fig. 5). The confocal images confirm the AF-647 loaded chitosan uniformly distributed in the Jurkat cells both in the cytosol as well as in the nucleus thereby confirming efficient delivery of the cargo to the targeted cells by chitosan nanoparticles. The flow cytometry data also support the confocal microscopy results with the cells exhibiting greater than 90% uptake of the chitosan nanoparticles. The superior uptake of the chitosan nanoparticles by cells may be attributed to the positive charges on the surface of chitosan that enable it to interact

Table 3
Release kinetics of saquinavir from drug loaded chitosan nanoparticles.

Kinetics model	pH 1.2		pH 5.5		pH 7.4		pH 9.0	
	k	R^2	k	R^2	k	R^2	k	R^2
Zero order(k_0)	8.998	0.4605	9.557	0.3964	2.189	0.9458	2.922	0.9188
First order (k_1)	0.3690	0.9533	0.490	0.9682	0.042	**0.9914**	0.0590	**0.9943**
Higuchi model (k_H)	29.139	0.9059	31.167	0.8780	12.726	0.9602	14.921	0.9798
Korsmeyer–Peppas (k_{KP})	40.514	0.9661	46.115	0.9716	6.541	**0.9901**	10.225	**0.9922**
Hixson–Crowell (k_{HC})	0.097	0.9141	0.1090	0.9153	0.012	**0.9973**	0.016	**0.9923**
Baker–Lonsdale(k_{BL})	0.029	0.9794	0.040	**0.9864**	0.004	0.9201	0.0061	0.9477
Weibull model (α)	1.510	**0.9982**	1.3580	**0.9992**	21.473	**0.9950**	50.132	**0.9972**
Hopfenberg model (k_{HB})	0.0001	0.9533	0.0001	0.9682	0.006	**0.9949**	0.0120	**0.9973**
Gompertz model (α)	0.8880	**0.9979**	0.7280	**0.9966**	8.6730	0.9704	21.039	0.9814

The bold letter signifies the best fit model for the drug release kinetics.

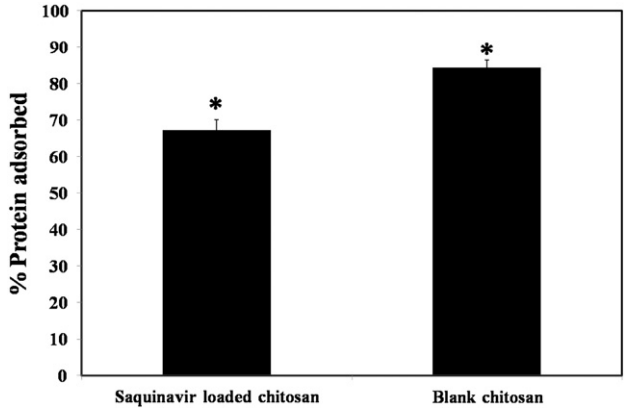

Fig. 4. Protein adsorption studies for Blank and saquinavir loaded chitosan after 12 h.

electrostatically with the negatively charged glycoproteins on the cell surface [40].

The cellular uptake of the drug loaded chitosan and free drug are shown in Fig. 5C. The cell uptake of the free drug was found to increase in a dose-dependent manner from 31 to 46%. In comparison, the cell uptake of the drug loaded chitosan nanoparticles was found to be nearly 2.5 times greater and ranged between 82% and 92% at the same drug concentrations. This confirms the finding that saquinavir loaded chitosan nanoparticles exhibit better cell uptake when compared with the free drug.

3.8. In vitro antiviral efficacy

Considering the superior cell targeting properties of the chitosan nanoparticles, we examined if the nanoparticles could deliver anti-HIV drugs to target T-cells with a greater targeting efficiency. A superior drug targeting efficiency could be beneficial by reducing the effective

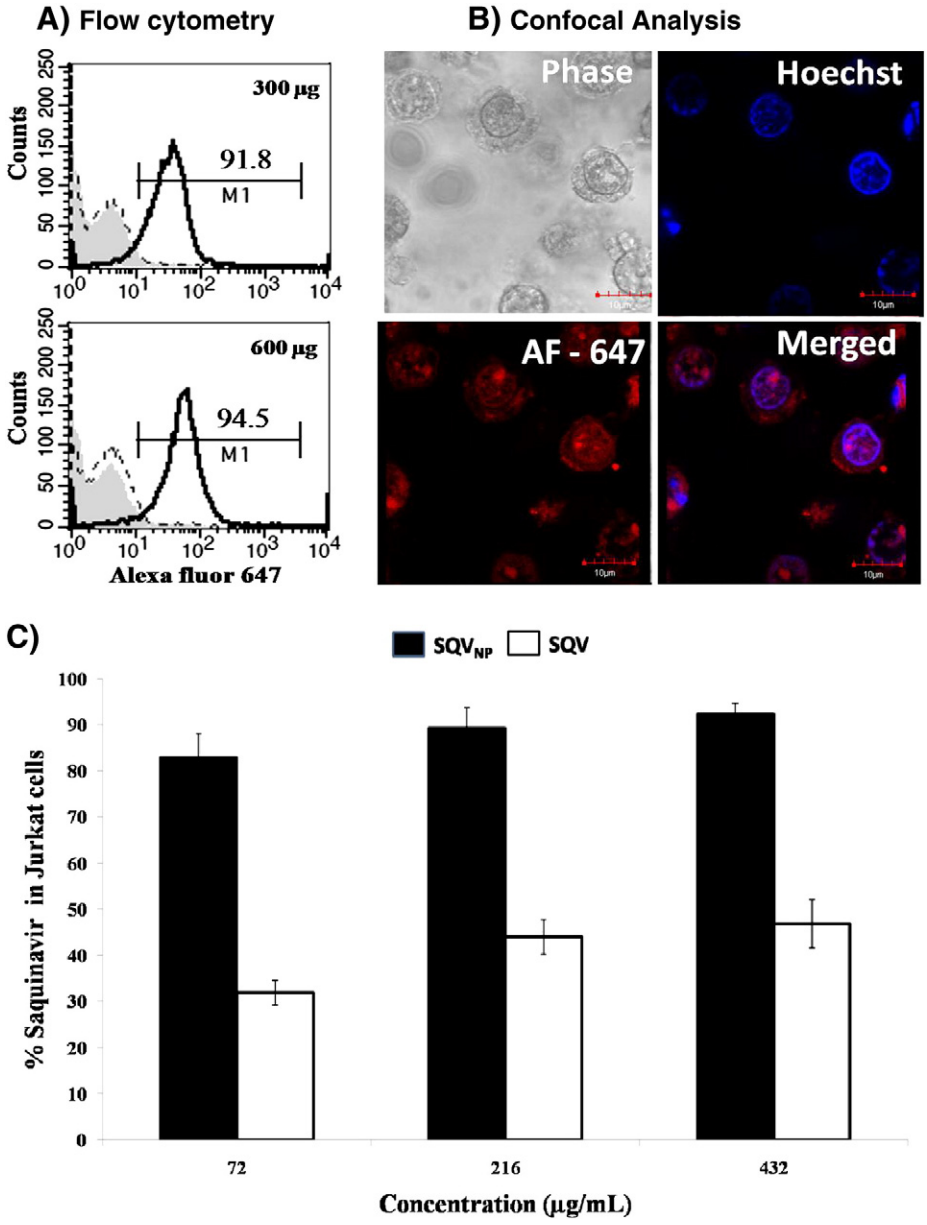

Fig. 5. Cell-targeting efficiency of the Alexa Fluor 647-loaded chitosan nanoparticles in Jurkat T-cells. A) Flow cytometry: cells were treated with plain or dye-loaded (300 or 600 µg) nanoparticles. The gray-filled histogram represents the cells unstained, the dashed line represents the cells stained with plain chitosan particles (PC) and the solid black line represents the cells stained with Alexa fluorophore-loaded (AFL) particles. The percentage of cells stained for the fluorophore is depicted above the marker. [B] Confocal images showing delivery of Alexa Fluor 647-loaded chitosan to Jurkat cells. Nuclear staining by Hoechst has been depicted in color blue and the red color represents Alexa Fluor 647 [C] cellular uptake of saquinavir loaded chitosan and plain saquinavir using Jurkat cell line. Dark bar represents the chitosan nanoparticles loaded with saquinavir (SQV_{NP}) and white bar represents the plain saquinavir (SQV).

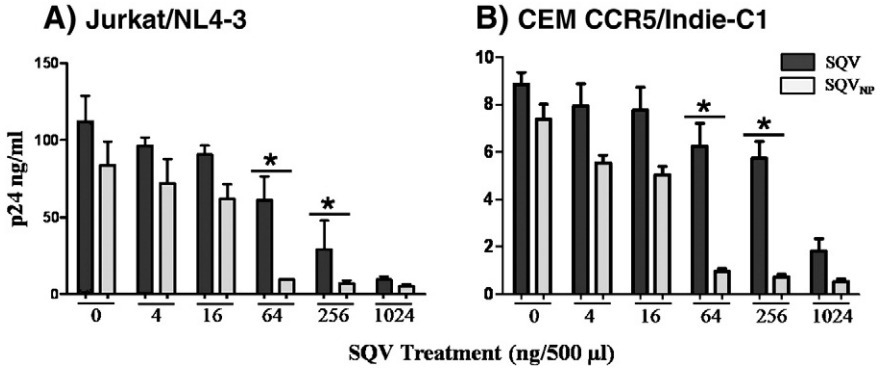

Fig. 6. The viral inhibition profiles of SQV and SQV$_{NP}$. (A) Jurkat T-cells or (B) CEM-CCR5 cells were treated with six different concentrations of soluble SQV (filled bars) or SQV$_{NP}$ (gray bars). In the SQV$_{NP}$ treatment, the chitosan concentration was normalized using blank chitosan nanoparticles. Jurkat and CEM-CCR5 cells were infected with NL4-3 and Indie-C1 viruses, respectively. The secretion of the viral antigen p24 into the medium was monitored using a commercial antigen-capture assay at 48 h following viral infection. An unpaired two-tailed *t*-test was performed using Graphpad Prism 5 software to determine the significance of differences in the magnitude of viral inhibition between two different groups (SQV and SQV$_{NP}$). Bars with $p < 0.05$ and $p < 0.01$ values represent significant inhibition of viruses in cells treated with SQV$_{NP}$ compared to SQV treatment. The data presented are from one of the two representative experiments.

drug dose required for comparable viral inhibition. Additionally, efficient drug delivery could also minimize the risk of drug resistance. We used two different molecular clones of HIV-1, NL4-3 and Indie-C1, representing two major genetic subtypes (subtypes B and C, respectively) in these assays and two different cell lines Jurkat and CEM-CCR5 both permissive for the virus as they express the primary receptor CD4. The Jurkat cells, expressing only the coreceptor CXCR4, but not CCR5, are permissive for the viral strains such as NL4-3. The Indie-C1 virus with a requirement for the coreceptor CCR5 in contrast cannot infect the Jurkat cells. The CEM-CCR5 cells naturally express CXCR4 and have been engineered to express human CCR5 on the surface. CEM-CCR5 cells therefore can be infected by both NL4-3 and Indie-C1 viral strains. In the assays, we used the Jurkat cells for the proliferation of NL4-3 and CEM-CCR5 cells for the proliferation of Indie-C1.

The T-cells in plain RPMI medium were first treated with varying concentrations of soluble SQV or with the nanoparticles loaded with an equivalent concentration of the drug (Fig. 6). Cells in the group treated with the nanoparticle were exposed to an equal concentration of chitosan by using blank chitosan nanoparticles for normalization. Saquinavir is a potent anti-retroviral agent that inhibits the viral protease efficiently and blocks viral maturation. After 30 min of incubation, cells were infected with 5 ng p24 equivalent of the virus and incubated for 6 more hours. After the infection, cells were washed thoroughly to remove residual virus, suspended in complete medium and incubated under controlled conditions. The amount of the virus secreted into the medium was monitored every 24 h up to 72 h and the viral core protein p24 was quantified using a commercial antigen-capture ELISA kit. The data obtained at 48 h are presented (Fig. 6).

In the absence of the drug, both the viruses proliferated efficiently in the target cells. In Jurkat cells, 111 ng of p24 was secreted from the NL4-3 infection in the absence of the drug. Indie-C1 on the other hand secreted only10 ng of p24 from the CEM-CCR5 cells as expected. The viral clone Indie-C1 does not proliferate to the same extent as NL4-3 in T-cells. When the viruses were treated with SQV, there was a progressive inhibition in the viral proliferation with increasing drug concentration. Importantly, SQV delivered to the T-cells through the nanoparticles inhibited viral proliferation at significantly lower concentrations as compared to the drug used in the soluble form, as is evident in both the virus-cell systems employed in the assay. For instance, in the CEM-CCR5/Indie-C1 model, in the presence of 64 ng/500 µl of soluble SQV, 6.25 ng/ml of p24 was secreted representing 28% of inhibition in viral proliferation. At the same concentration of the drug delivered as nanoparticle, only 0.96 ng/ml of p24 was secreted representing 82% of inhibition which is a significantly superior viral inhibition compared to that of the soluble drug. Comparable results were obtained at other drug concentrations, other time points (data not shown) and in the Jurkat/NL4-3 model. Collectively, the data are suggestive of an increased efficiency in drug delivery resulting in a significant viral inhibition when SQV was delivered through the chitosan nanoparticles. The enhanced reduction in the viral load from 64 ng/500 µl onwards for the saquinavir-loaded chitosan nanoparticles may be attributed to their better cell uptake when compared with the free drug.

4. Conclusion

Chitosan nanogels between 10 and 200 nm were prepared using the ionic gelation technique and 72% encapsulation of the protease inhibitor saquinavir was achieved. Maximum swelling was observed in acidic pH where maximum drug release also occurred. The drug loaded chitosan showed a slight reduction in serum protein adsorption without compromising on the cell uptake. The saquinavir loaded chitosan nanoparticles were found to exhibit superior potency than the free drug even in nanogram levels. Both strains of HIV – NL4-3 and Indie-C1 - were found to respond to chitosan containing saquinavir indicating the potency of this system as an effective anti-HIV system.

Acknowledgements

The authors acknowledge the financial support from ICMR (No. 35/9/2009-BMS) and SASTRA University and JNCASR for the infrastructural support.

References

[1] P. Piot, M. Bartos, P.D. Ghys, N. Walker, S. Bernhard, The global impact of HIV/AIDS, Nature 410 (2001) 968–973.
[2] J.D. Neves, et al., Nanotechnology-based system for the treatment and prevention of HIV/AIDS, Adv. Drug Deliv. Rev. 62 (2010) 458–477.
[3] H.L. Wong, et al., Nanotechnology application for improved delivery of antiretroviral drugs to the brain, Adv. Drug Deliv. Rev. 62 (2010) 503–517.
[4] U. Gupta, N.K. Jain, Non-polymeric nano-carriers in HIV/AIDS drug delivering and targeting, Adv. Drug Deliv. Rev. 62 (2010) 478–490.
[5] J.T. Radonna, S.E.C. Yie, H.Y. Fay, E.V. Susan, Mutagenesis of protease cleavage sites in the HIV type 1 *gag*polyprotein, J. Virol. 65 (1991) 922–930.
[6] D.K. Jardine, et al., Effect of protease inhibitors on HIV-1 maturation and infectivity, Antiviral Res. 45 (2000) 59–68.
[7] X. Li, W.K. Chan, Transport, metabolism and elimination mechanism of anti-HIV agents, Adv. Drug Deliv. Rev. 39 (1999) 81–103.
[8] E.K. Annice, et al., Saquinavir, an HIV protease inhibitor, is transported by P-glycoprotein, J. Pharmacol. Exp. Ther. 286 (1998) 1439–1445.
[9] B.K. Richard, et al., The drug transporter P-glycoprotein limits oral absorption and brain entry of HIV-1 protease inhibitors, J. Clin. Invest. 101 (1998) 289–294.
[10] K.E. Thummel, et al., Enzyme-catalyzed process of first hepatic and intestinal drug extraction, Adv. Drug Deliv. Rev. 27 (1997) 99–127.
[11] S. Jonathan, et al., The effect of high dose saquinavir on viral load and CD4$^+$ T-cell counts in HIV infected patients, Ann. Intern. Med. 124 (1996) 1039–1050.

[12] T. Dutta, K.J. Narendra, Targeting potential and anti-HIV activity of lamivudine loaded mannosylated poly (propyleneimine) dendrimer, Biochim. Biophys. Acta 1770 (2007) 681–686.
[13] E. Pretzer, et al., Inhibition of HIV-1 infection of macrophage and H9 cells by free or liposome encapsulated L-689,502, an inhibitor of the viral protease, Antiviral Res. 26 (1995) A358.
[14] L. Yang, et al., Synthesis, nanosizing and in vitro drug release of a novel anti-HIV polymeric prodrug: chitosan-O-isopropyl-5′-O-d4T monophosphate conjugate, Bioorg. Med. Chem. 18 (2010) 117–123.
[15] Y.C. Kuo, et al., Entrapment and release of saquinavir using novel cationic solid lipid nanoparticles, Int. J. Pharm. 1–2 (2009) 206–213.
[16] L.K. Shah, et al., Intracellular delivery of saquinavir in biodegradable polymeric nanoparticles for HIV/AIDS, Pharm. Res. 23 (2006) 2638–2645.
[17] G. XU, et al., Bioconjugated quantum rods as targeted probes for efficient transmigration across an in vitro blood–brain barrier, Bioconjug. Chem. 19 (2008) 1179–1185.
[18] T.K. Vyas, et al., Improved oral bioavailability and brain transport of saquinavir upon administration in novel nanoemulsion formulations, Int. J. Pharm. 347 (2008) 93–101.
[19] H. Boudad, et al., Combined hydroxylpropyl-β-cyclodextrin and poly(alkyl cyanoacrylate) intended for oral administration of saquinavir, Int. J. Pharm. 218 (2001) 113–124.
[20] P. Sharma, et al., Novel drug delivery approaches on antiviral and antiretroviral agents, J. Adv. Pharm. Technol. Res. 3 (2012) 147–159.
[21] L.N. Ramana, et al., Investigation on the stability of saquinavir loaded liposomes: implication on stealth, release characteristics and cytotoxicity, Int. J. Pharm. 431 (2012) 120–129.
[22] Y. Yang, et al., Porcine interleukin-2 gene encapsulated in chitosan nanoparticles enhances immune response of mice to piglet paratyphoid vaccine, Comp. Immunol. Microbiol. Infect. Dis. 30 (2007) 19–32.
[23] B. Johan, T. Pentii, Blood protein adsorption onto chitosan, Biomaterials 23 (2002) 2561–2568.
[24] H.P. Jae, et al., Targeted delivery of low molecular drugs using chitosan and its derivatives, Adv. Drug Deliv. Rev. 62 (2010) 28–41.
[25] S. Gunaseelan, et al., Synthesis of PEG-based saquinavir prodrug conjugates and assessment of release and Anti-HIV-1 bioactivity using a novel protease inhibition assay, Bioconjug. Chem. 15 (2004) 1322–1333.
[26] R. Merlin, S. Pulavendran, C. Rose, A.B. Mandal, Chitosan nanoparticles as dual growth factor delivery system for tissue engineering applications, Int. J. Pharm. 410 (2011) 145–152.
[27] H. Meringo, A. Zou, Y. Chengli, Z. Yong, Z. Jianping, W. Jing, Z. Qinny, L. Jing, Z. Qiang, Somatostatin receptor-mediated tumor-targeting drug delivery using octreotide-PEG-deoxycholic acid conjugate-modified N-deoxycholic acid-O, N-hydroxyethylation chitosan micelles, Biomaterials 33 (2012) 6393–6407.
[28] K. Lalita, Y. Rangrong, Preparation, characterization and in vitro release study of carvacrol loaded chitosan nanoparticles, Colloids Surf. B 84 (2011) 163–171.
[29] V. Jain, et al., Preparation and performance evaluation of saquinavir laden cationic submicron emulsions, Drug Deliv. 16 (2009) 37–44.
[30] R.S. Mohammad, M.T. Roya, M. Abel, A.R. Mohammad, Synthesis and characterization of biodegradable chitosan beads as nano-carriers for local delivery of satranidazole, Carbohydr. Polym. 81 (2010) 726–731.
[31] A. Jain, et al., Design and development of ligand-appended polysaccharidic nanoparticles for the delivery of oxaliplatin in colorectal cancer, Nanomed. Nanotechnol. 6 (2010) 179–190.
[32] J. Liu, et al., Novel pH-sensitive chitosan-derived micelles loaded with paclitaxel, Carbohydr. Polym. 82 (2010) 432–439.
[33] L.T. Min, et al., The storage stability of chitosan/tripolyphosphate nanoparticles in a phosphate buffer, Carbohydr. Polym. 84 (2011) 756–761.
[34] Q. Yuvan, et al., Controlled and extended drug release behavior of chitosan based nanoparticle carrier, Acta Biomater. 6 (2010) 1140–1148.
[35] Mourya, et al., Trimethyl chitosan and its applications in drug delivery, J. Mater. Sci. 20 (2009) 1057–1079.
[36] Y.C. Kuo, C.C. Wang, Cationic solid lipid nanoparticles with primary and quaternary amines for release of saquinavir and biocompatibility with endothelia, Colloids Surf. B 101 (2013) 101–105.
[37] A. Anitha, et al., Preparation, charaterisation, in vitro drug release and biological studies of curcumin loaded dextran sulphate–chitosan nanoparticles, Carbohydr. Polym. 84 (2011) 1158–1164.
[38] G. Li, et al., Induction of Th1-type immune response by chitosan nanoparticles containing plasmid DNA encoding house dust mite allergen Der p 2 for oral vaccination in mice, Cell. Mol. Immunol. 6 (2009) 45–50.
[39] X. Li, et al., Interaction of bovine serum albumin with self assembled nanoparticles of modified chitosan 6-O-cholesterol, Colloids Surf. B 92 (2012) 136–141.
[40] V.T. Marchesi, et al., Chemical characterization and surface orientation of the major glycoprotein of the human erythrocyte membrane, Proc. Natl. Acad. Sci. U. S. A. 69 (1972) 1445–1449.